RESTORATION OF BIOMEDICAL IMAGES USING LOCALLY ADAPTIVE B-SPLINE SMOOTHING

Xabier Artaechevarria, Arrate Muñoz-Barrutia, Carlos Ortiz-de-Solorzano

Oncology Division, Centre for Applied Medical Research (CIMA), University of Navarra, Pamplona, Spain
Dep. of Electrical, Electronic and Control Eng., University of Navarra (TECNUN), San Sebastián, Spain

ABSTRACT

In this paper we present an adaptive B-spline smoothing algorithm to reduce noise in biomedical images. The filter consists of a convolution between the input image and an adaptive B-spline kernel that varies its size according to the local image characteristics. We show that this filter can be efficiently implemented by taking advantage of the convolution and factorization properties of B-splines. We tested our filter on phantoms and real images, obtaining very high noise reduction in homogeneous areas with little degradation of the edges.

Keywords: biomedical images, restoration, B-splines, scale-scene.

1. INTRODUCTION

The presence of noise is a common characteristic of virtually all biomedical images. Noise can be of different types and magnitudes, depending on the imaging modality and the particular acquisition conditions. Two examples of biomedical images are magnetic resonance imaging (MRI) and small animal X-ray computed tomography (micro-CT). In MRI, there exists a trade-off between resolution and Rician noise. The standard protocols for image acquisition with micro-CT use low-dose X-rays and a moderate number of projections for the reconstruction, resulting in images with considerable noise, which can be modeled as Gaussian, and circle shaped artifacts. Thus, the need arises for efficient noise filtering and image enhancement strategies, as pre-processing steps prior to any high level segmentation or image understanding task. A key requirement of these filters is that they must remove noise without losing any relevant information contained in the image. A number of different approaches have been described in the literature during the past two decades. Among them, an interesting class of filters relies on the convolution of the image with scaled kernels [1]. In other words, the size of the kernel at each image position matches the underlying image characteristics; i.e., wide kernels are used in smooth regions and narrow ones in edges and highly textured areas of the image. The common drawback of this type of algorithms is that the computational complexity of the filter depends on the size of the convolution kernel and it can be quite high on average.

In this paper, we present an adaptive smoothing method with a fixed -scale independent- computational load. It uses an estimate of the scale calculated at each pixel. This controls the size of the B-spline kernel to be convolved at that position. The filter is applied to micro-CT and MRI images with satisfactory results.

This project was partially funded through the UTE project CIMA. X. Artaechevarria is funded by a predoctoral scholarship of the Basque Government. A. Muñoz-Barrutia holds a Ramón y Cajal fellowship of the Spanish Ministry of Science and Technology. C. Ortiz-de-Solórzano is currently supported by the Spanish Ministry of Science and Education (MCYT TEC2005-04732), the EU Marie Curie Program (MIRG-CT-2005-028342) and a Ramón y Cajal Fellowship.

2. ADAPTIVE FILTERING ALGORITHM

In this section, we first describe the scale computation algorithm and then we derive an exact and efficient B-spline filtering method.

2.1. Scale Computation

Our local scale estimation is based on a method described in [1]: for each pixel, a hyper-ball grows until a certain inhomogeneity criterion is fulfilled. This criterion can be adjusted depending on the expected noise level and the degree of detail wanted in the image. In presence of diffuse borders, normally caused by motion artifacts, non-zero scale values might be estimated for pixels located at edges. That would lead to unwanted diffusion of the edges. For that reason, we added an extra step to the algorithm that detects this kind of borders and forces the scale value to be null on them.

2.2. Scale-Based B-spline Filtering

We describe now the derivation of a general and efficient scale-based B-spline filtering algorithm for bivariate functions. The smoothed discrete output $f_{\mathbf{O}}(\mathbf{b})$ at position $\mathbf{b} \in \mathbb{Z}^2$ is calculated as the convolution of the input function $f_{\mathbf{I}}(\mathbf{x})$, $\mathbf{x} \in \mathbb{R}^2$ with a B-spline kernel $\beta^{n_2}\left(\frac{\mathbf{x}}{a}\right)$ evaluated at $\mathbf{b}$

$$f_{\mathbf{O}}(\mathbf{b}) = \left(f_{\mathbf{I}}(\cdot) * \beta^{n_2}\left(\frac{\cdot}{a}\right)\right)(\mathbf{b}). \quad (1)$$

2.2.1. Operators and definitions

We introduce some operators and definitions that will be helpful to solve our problem. The scaled-centered B-spline can be defined as a 2D extension of the one given in [2]:

$$\frac{1}{a^2}\beta^{n_2}\left(\frac{\mathbf{x}}{a}\right) = \Delta_a^{n_2+1} * \frac{1}{a^{2n_2+2}} D^{-(n_2+1)}\delta(\mathbf{x}+\mathbf{s}_{a,n_2}) \quad (2)$$

where $\Delta_a^{n_2+1}(\mathbf{x})$ are the expanded finite differences given by

$$\Delta_a^{n_2+1}(\mathbf{x}) = \sum_{\mathbf{k}\in(0,0)}^{(n_2+1,n_2+1)} q(\mathbf{k})\delta(\mathbf{x}-a\mathbf{k})$$

with $\mathbf{k}=(k_1,k_2)$, $q(\mathbf{k})=\prod_{i=1}^{2} q(k_i)$ and $q(k_i)=\binom{n_2+1}{k_i}(-1)^{k_i}$, D^{-1} is the continuous integral operator defined as

$$D^{-1}h(x_1,x_2) = \int_{-\infty}^{v_1}\int_{-\infty}^{v_2} h(v_1,v_2)dv_1dv_2$$

and $\mathbf{s}_{a,n_2} = a\frac{n_2+1}{2}(1,1)$ is a shift required to center the B-spline. Besides, we have that the integral of a B-spline is given by the following expression [2]:

$$D^{-(n_2+1)}\beta^{n_1}(\mathbf{x}) = \left(\Delta_1^{-(n_2+1)} * \beta^{n_1+n_2+1}\right)(\mathbf{x}-\mathbf{s}_{1,n_1}) \quad (3)$$

where $\Delta_{\mathbf{1}}^{-1}$ is the inverse finite-difference operator that can be efficiently implemented by recursive filtering.

2.2.2. Derivation of the Algorithm

Using (1) and (2) , we can express the smoothing of an arbitrary continuous function $f_{\mathbf{i}}(\mathbf{x})$ as the mixed convolution

$$f_{\mathbf{o}}(\mathbf{b}) = \frac{1}{a^{2n_2}}\left(\Delta_a^{n_2+1} * v\right)(\mathbf{b}), \quad (4)$$

where the (n_2+1)-integral of $f_{\mathbf{i}}(\mathbf{x})$ is given by

$$v(\mathbf{x}) = D^{-(n_2+1)} f_{\mathbf{i}}(\mathbf{x}+\mathbf{s}_{a,n_2}). \quad (5)$$

At this point, we adopt a continuous domain formulation by interpolating the input discrete image samples $f_{\mathbf{i}}[\mathbf{k}]$, $\mathbf{k}\in\mathbb{Z}^2$ and expressing them on a B-spline basis resulting in the 2D box-spline $f_{\mathbf{i}}(\mathbf{x})$. Thus, we have $f_{\mathbf{i}}(\mathbf{x}) = (c_\delta * \beta^{n_1})(\mathbf{x})$ where $c_\delta(\mathbf{x}) = \sum_{k\in Z} c[\mathbf{k}]\delta(\mathbf{x}-\mathbf{k})$ are the B-spline interpolation coefficients calculated as in [3]. We can then substitute the 2D box-spline model on equation (4) and use the integral equivalence (3) to finally obtain

$$f_{\mathbf{o}}(\mathbf{b}) = \sum_{\mathbf{k}\in(0,0)}^{(M-1,M-1)} g[\mathbf{b}-\mathbf{k}]w_a(\mathbf{k})$$

where $g_\delta = \Delta_1^{-(n_2+1)} * c_\delta$ are the (n_2+1)-times integrated B-spline coefficients,

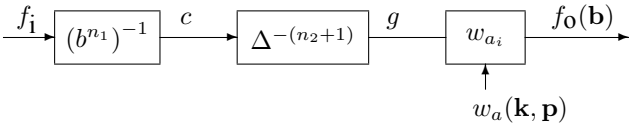

Fig. 1. Schematic representation of the locally adaptive smoothing algorithm.

$$w_a(\mathbf{k}) = \left(\frac{1}{a^{2n_2}}\Delta_a^{n_2+1}(\cdot) * \beta^{n_1+n_2+1}(\cdot+\mathbf{s}_{a-1,n_2})\right)(\mathbf{k}) \quad (6)$$

is a 2D non-separable mask that corresponds to the (n_2+1)-finite differences of a shifted B-spline of degree (n_1+n_2+1) and $M=(n_1+n_2+1+a(n_2+1))$ is the mask size per dimension.

The spatial structure of the filter w_a has particular properties. As the convolution with the scaled finite differences results in the replication of the sampled B-spline with a distance a between replicas, the mask corresponds to a modified *'a trous'* filter. Smoothing at each position $\mathbf{b}$ is done by filtering of the coefficients g_δ with $(n_2+2)^2$ *'clusters'* of size $(n_1+n_2+1)^2$, each *'cluster'* being separated from its neighbors by a distance a in both dimensions. Consequently, the maximum number of non-null weights of the filter mask is equal to $(n_2+2)^2\cdot(n_1+n_2+1)^2$. Finally, when the scale is smaller than the cluster size $a<(n_1+n_2+1)$, the clusters overlap, and the most efficient approach is to calculate the convolution with the full mask. For moderate and large scale values $a\geq(n_1+n_2+1)$, the most efficient option is to write the computation as the inner product of g_δ and a series of pre-calculated non-null weights w_a given by the following equation

$$f(\mathbf{b}) = \sum_{\mathbf{k}=(0,0)}^{(n_2+1,n_2+1)}\ \sum_{\mathbf{p}=(0,0)}^{(N-1,N-1)} g_\delta[\mathbf{p}+\mathbf{p}_0+\mathbf{b}]w_a(\mathbf{k},\mathbf{p}) \quad (7)$$

where $N=n_1+n_2+1$, $\mathbf{p}_0+\mathbf{b}$ is the first significant element of g_δ for each $\mathbf{k}$, $\mathbf{p}_0=\lceil -a\mathbf{k}+\mathbf{s}_{a-2,n_2}+\mathbf{s}_{1,n_1}\rceil$ and w_a is the following look-up table

$$w_a(\mathbf{k},\mathbf{p}) = \frac{1}{a^{2n_2}}q(\mathbf{k})\beta^{n_1+n_2+1}(-a\mathbf{k}-\mathbf{p}-\mathbf{p}_0+\mathbf{s}_{a-1,n_2}) \quad (8)$$

2.2.3. Fast Implementation

A box diagram for a fast implementation of the algorithm is shown in Figure 1. For each of the scales, we compute the most reduced set of non-null weights w_a, given by (6) when $a<(n_1+n_2+1)$ and by (8) if $a\geq(n_1+n_2+1)$. We then store the weight values in a look-up table. In the initialization step, the B-spline expansion coefficients c_δ of the sample image $f_{\mathbf{i}}(\mathbf{x})$ are calculated, and the running sum operator $\Delta_{\mathbf{1}}^{-1}$ is applied (n_2+1)-times. The intermediate result g_δ does not depend on the scale a. The output $f_{\mathbf{o}}(\mathbf{b})$ at position $\mathbf{b}$ is calculated by filtering with the modified *'a trous'* filter whose coefficients are stored in the matrix w_a.

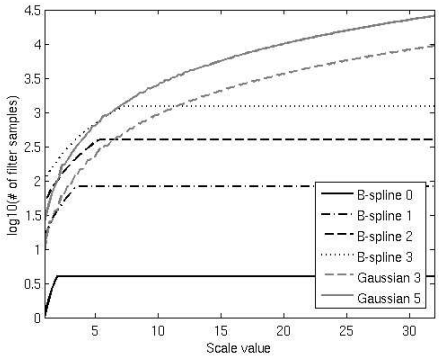

Fig. 2. Number of samples of the filter (log scale) versus the scale value.

Figure 2 illustrates the important reduction in the number of filter samples, and therefore in computational cost, obtained at medium and high scales by our adaptive B-spline filter implementation (black lines) when compared with a sampled Gaussian kernel with a sigma equal to the scale value ($\sigma = a$) (gray-curves). Values are shown for different B-splines degrees (i.e., $n_2 = 0, ..., 3$) and for two typical Gaussian kernel sizes (i.e., $\lceil 3\sigma \rceil$ and $\lceil 5\sigma \rceil$).

3. EXPERIMENTAL RESULTS

Our filter was evaluated and compared to other commonly used filters both qualitatively and quantitatively. For the quantitative analysis, we used the Shepp-Logan phantom, with two different kinds of noise and artifacts. First, we modified the intensities of the phantom so that it followed a Rician distribution, as real MRI magnitude images do. Alternatively, we reconstructed the phantom image from a limited number of projections using a filtered back-projection algorithm, imitating the micro-CT image acquisition process. The performance was evaluated looking at two different parameters: residual noise (RN), which is the standard deviation of pixel intensities in homogeneous areas of the image [1], and average edge width (AEW), calculated as the ratio between the total number of pixels that belong to an edge and the number of edges in the image [4]. In particular, our filter was compared to fixed scale smoothing and anisotropic diffusion [5]. The possible scale values for the B-spline adaptive smoothing were integer values between 0 and 15. The scale value for the fixed scale smoothing was set to 10, which was approximately the mean scale value for the phantom. In all cases, linear B-splines were used. The parameters for the anisotropic diffusion were typical: 0.1 time step, 10 iterations and 3.0 conductance.

Table 1 shows the mean and standard deviation of the RN values in 23 manually selected homogeneous regions of the phantom, for three different levels of Rician (MRI-like) noise (σ of 500, 1000 and 1500 for the underlying Gaussian distributions). The mean AEW values for the three filters compared are shown in Table 2. Tables 3 and 4 show the results

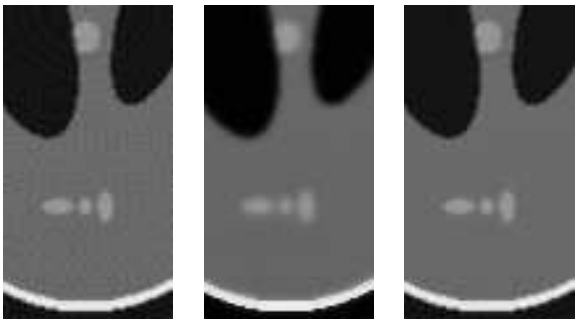

(a) (b) (c)

Fig. 3. (a) Detail of Shepp-Logan phantom reconstructed from 128 projections. (b) Phantom after diffusive filtering. (c) Phantom after adaptive B-spline smoothing.

on the Shepp-Logan phantom with the micro-CT-like noise and artifacts. In all cases, it is clear that our adaptive B-spline smoothing outperforms fixed scale smoothing and anisotropic diffusion, since it provides higher homogeneity and better defined edges simultaneously. When compared to anisotropic diffusion, the average improvement in homogeneity is 54% for the MR phantom and 43% for the micro-CT one, with a reduction in AEW of 0.73 and 1.08 pixels respectively. The mentioned difference in homogeneity is statistically significant ($p < 0.001$), as shown using a Wilcoxon matched-pairs signed-rank test. The effect can be qualitatively observed in Figure 3, where the two filters are applied to the phantom reconstructed from 128 projections.

We then tested our filter on real biomedical images. Figure 4 shows an MR image of the human head. We found that, for a comparable level of smoothing in homogeneous areas, adaptive B-spline filtering blurs borders considerably less than the other filters. The same effect can be observed in Figure 5, which shows a micro-CT image of a mouse lung with multiple small details, as tumors and vessels.

	NF	FS	AD	BS
Level 1	451.57	431.00	194.92	**67.92**
	78.24	472.85	201.46	**25.57**
Level 2	920.10	445.40	253.09	**124.90**
	153.06	441.85	170.97	**42.15**
Level 3	1346.66	477.19	343.47	**181.05**
	240.38	416.97	152.42	**54.32**

Table 1. Mean (first entry) and standard deviation (second entry) of RN values for different levels of Rician noise and denoising filter: NF: No filtering; FS: Fixed-scale B-spline; AD: Anisotropic diffusion; BS: Adaptive B-spline.

	NF	FS	AD	BS
Mean AEW	7.54	11.33	8.34	**7.61**

Table 2. Mean AEW values averaged through the three different levels of rician noise for different denoising filters

	NF	FS	AD	BS
128 Pr.	1106.66	398.98	220.88	**134.51**
	61.45	422.15	210.63	**120.08**
256 Pr.	648.04	423.00	221.95	**124.53**
	60.82	449.15	228.95	**110.72**
512 Pr.	499.26	428.84	222.16	**121.96**
	67.93	456.53	233.73	**109.48**

Table 3. Mean (first entry) and standard deviation (second entry) of RN values for different number of projections and denoising filter: NF: No filtering; FS: Fixed-scale B-spline; AD: Anisotropic diffusion; BS: Adaptive B-spline.

	NF	FS	AD	BS
Mean AEW	8.28	9.77	9.50	**8.42**

Table 4. Mean AEW values averaged through the three different numbers of projections for different denoising filters

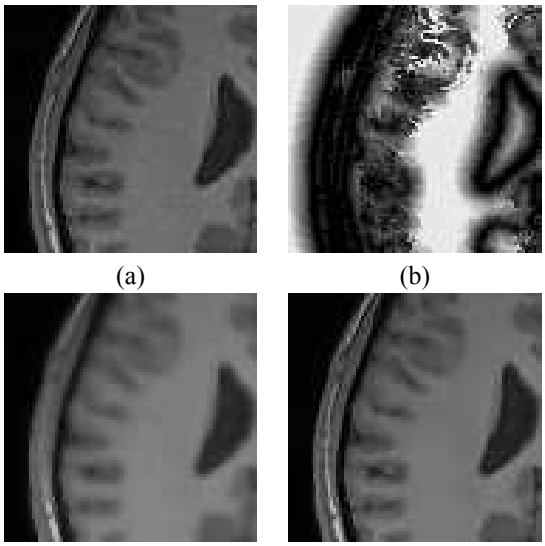

Fig. 4. (a) Region of MR image of human head. (b) Scale image that corresponds to (a). (c) Same region after diffusive filtering. (d) Same region after adaptive B-spline smoothing.

4. CONCLUSIONS

We showed that scale-based B-Spline filtering can yield satisfactory results in biomedical images of different modalities and different levels of noise. In our experiments, adaptive B-spline smoothing provided a better trade-off between removal of noise and edge degradation than anisotropic diffusion. This is an important property that may simplify further image processing and analysis, such as segmentation of organs or diseased areas. Moreover, the computational load of the filter is independent of the scale value and depends only on the B-spline order selected for interpolation and convolution, which is an advantage over other scale-based filters.

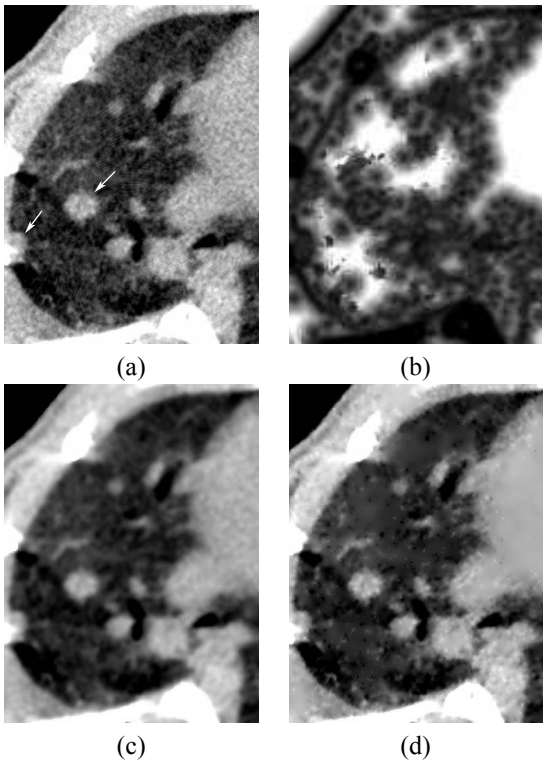

Fig. 5. (a) Left region of a micro-CT image of a mice lung with a moderate tumor load (white arrows indicate tumors). (b) Scale-scene that corresponds to (a). (c) Same region after diffusive filtering. (d) Same region after adaptive B-spline smoothing.

5. REFERENCES

[1] P.K. Saha and J.K. Udupa, "Scale-Based Diffusive Image Filtering Preserving Boundary Sharpness and Fine Structures", *IEEE Trans. on Medical Imag.*, vol. 20, no. 11, pp. 1140-1155, Nov. 2001.

[2] A. Muñoz-Barrutia, R. Ertlé and M. Unser, "Continuous Wavelet Transform with Arbitrary Scales and $O(N)$ Complexity", *Signal Proc.*, vol. 82, no. 5, pp 749-757, May 2002.

[3] M. Unser, "Splines, A Perfect Fit for Signal and Image Processing", *IEEE Signal Proc. Mag.*, vol. 16, no. 6, pp. 22-38, Nov. 1999.

[4] P. Marziliano, F. Dufaux, S. Winkler, and T. Ebrahimi, "A No-reference Perceptual Blur Metric", *Proc. of the Int. Conf. on Image Proc.*, vol. 3, pp 57-60, Sept. 22-25, 2002.

[5] P. Perona and J. Malik, "Scale-Space and Edge Detection using Anisotropic Filtering", *IEEE Trans. Pattern Anal. Machine Intell.*, vol. 12, no. 7, pp 629-639, July 1990.